UNSTEADY ROTATING ELECTROOSMOTIC FLOW THROUGH A SLIT MICROCHANNEL

D.-Q. Si **Y.-J. Jian***

School of Mathematical Science
Inner Mongolia University
Hohhot, China

L. Chang

School of Mathematics and Statistics
Inner Mongolia University of Finance and Economics
Hohhot, China

Q.-S. Liu

School of Mathematical Science
Inner Mongolia University
Hohhot, China

ABSTRACT

Using the method of Laplace transform, an analytical solution of unsteady rotating electroosmotic flow (EOF) through a parallel plate microchannel is presented. The analysis is based upon the linearized Poisson-Boltzmann equation describing electrical potential distribution and the Navies Stokes equation representing flow field in the rotating coordinate system. The discrepancy of present problem from classical EOF is that the velocity fields are two-dimensional. The rotating EOF velocity profile and flow rate greatly depend on time t, rotating parameter ω and the electrokinetic width K (ratio of half height of microchannel to thickness of electric double layer). The influence of the above dimensionless parameters on transient EOF velocity, volume flow rate and EO spiral is investigated.

Keywords: Unsteady, Rotating electroosmotic flow (EOF), Laplace transform method.

1. INTRODUCTION

Microfluidics plays an important role in micro-electro-mechanical-systems (MEMS) because of its potential applications as a tool for studying fundamental physical and biochemical processes and a platform for performing biological and chemical assays [1-3]. When a microchannel wall keeps in contact with an electrolyte, a thin electric double layer (EDL) will be formed adjacent to the solid surface. Characteristic thickness of the EDL is commonly known as the Debye length. On application of the axial electric field, the positive ions (cations) in the electrolyte move toward the cathode and the negative ions (anions) toward the anode. The adjacent and bulk liquid phase will be carried by the migration of the mobile ions due to viscosity, resulting in an electroosmotic flow (EOF). Comparing to conventional pressure driven flow, EOF has many advantages such as absence of mechanical parts, less convective dispersion, ease of control, high reliability and no noise.

Experimental, numerical and theoretical researches of steady EOF have been investigated in different geometric domains such as slit parallel plates [4], cylindrical capillary [5,6], annulus [7,8], elliptical pore [9], rectangular [10-13], T-shape [14], semicircular [15] and sector [16] microchannel cross-sections. Time-dependent EOF has been focused increasing attention as an alternative mechanism of microfluidic transport. Keh and Tseng [17] studied transient EOF in a one dimensional capillary, and derived closed-form solutions for the transient EOF velocity and flow rate. Kang *et al.* [18] analyzed transient EOF field in cylindrical microchannels using Green's function method. Sun *et al.* [19] researched the thermally fully developed EOF of power-law fluids in a circular microchannel. Moreover, the fluid rheological behavior usually needs to be considered in practical applications. Many investigations associated with the EOF of non-Newtonian fluids, such as Jeffrey [20], generalized Maxwell [21-23] and power-law [24] fluids through microchannel were studied.

Rotating flow play an essential role in classical fluid mechanics. Li *et al.* [25] presented the rotating EOF of third grade fluids between two microparallel plates by employing the perturbation method; Xie *et al.* [26] analyzed the rotating EOF of power-law fluids at high zeta potential. Recently, the transient rotating Electromagnetohydrodynamic micropumps between two infinite microparallel plates was researched by Jian

* Corresponding author (jianyj@imu.edu.cn)

DOI : 10.1017/jmech.2016.9
Copyright © 2016 The Society of Theoretical and Applied Mechanics
https://doi.org/10.1017/jmech.2016.9 Published online by Cambridge University Press

et al. [27]. Using linearized Poisson-Boltzmann equation and the modified Navier-Stokes equation by using Coriolis force, Chang and Wang [28] developed a steady rotating EOF through microparallel plates. They obtained steady analytical solutions of rotating EOF velocity and volume flow rate. However, the investigation of the transient process of this problem is still open. In this article, we will study the transient rotating EOF by the method of Laplace transform. The dependence of unsteady rotating EOF velocity and volume flow rate on time t, rotating frequency ω and electrokinetic width K will be discussed.

2. ANALYSIS OF THE PROBLEM

The transient rotating EOF of incompressible viscous fluids between two negatively charged microparallel plates is studied. The physical problem and selection of coordinate system are sketched in Fig. 1, where x^*-axis and y^*-axis are tangential to the charged surface and z^*-axis is perpendicular to the x^*y^*plane. The height of the channel is $2H$, while the channel centerline is assumed to be oriented along the x^*-axis. The electric field is applied along the x^*-axial direction. The whole system rotates about the z^*-axis with angular velocity Ω. In the following expressions, the variables with prime denote dimensional, while the ones without a prime are non-dimensional.

2.1 The Electrical Potential Distribution

For low electric potential on the plates, the Debye-Hückel approximation can be used in Poisson-Boltzmann equation. For a symmetric electrolyte, the electric potential ψ^* is given

$$\frac{d^2\psi^*}{dz^{*2}} = \kappa^2\psi^* \ , \ \text{where} \ , \ \kappa^2 = 2n_0 z_0{}^2 e^2 / \varepsilon k_B T \ , \tag{1}$$

here κ is Debye-Hückel parameter, and its inverse $1/\kappa$ is called Debye length or the thickness of EDL, n_0 is the ion density of bulk liquid, ε is the dielectric constant of the electrolyte liquid, e is the electron charge, z_0 is the valence, k_B is the Boltzmann constant and T is the absolute temperature. The boundary conditions for electrical potential are

$$\psi^*(z^*)|_{z^*=H} = \zeta \ , \tag{2}$$

$$\psi^*(z^*)|_{z^*=-H} = \zeta \ , \tag{3}$$

where ζ is the wall zeta potential. Introducing the following dimensionless variables

$$\psi = \psi^* / \zeta \ , \ z = z^* / H \ , \ K = \kappa H \ , \tag{4}$$

where K is called electrokinetic width and means ratio of half height of microchannel to thickness of EDL. Dimensionless electrical potential Eq. (1) and corresponding boundary conditions (2) and (3) can be written as

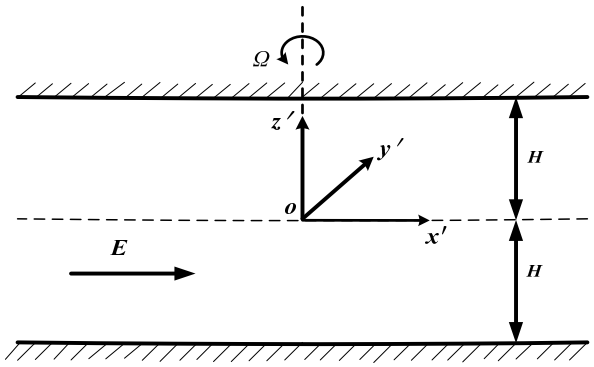


Fig. 1 Schematic of rotating EOF between two infinite microparallel plates.

$$\frac{d^2\psi}{dz^2} = K^2\psi \ , \tag{5}$$

$$\psi(z)|_{z=1} = 1 \ , \tag{6}$$

$$\psi(z)|_{z=-1} = 1 \ , \tag{7}$$

The solution of the above problem takes the form

$$\psi = \cosh(Kz) / \cosh K \ . \tag{8}$$

2.2 Analytical Solutions of Velocity and Flow Rate

In a rotating frame with angular velocity Ω in z^* direction, pressure gradient, Coriolis force, viscous force and body force due to electric field should be involved in Navier-Stokes equation [28]

$$\rho\left(\frac{\partial\vec{u}^*}{\partial t^*} + \vec{u}^*\cdot\nabla^*\vec{u}^* + 2\vec{\Omega}\times\vec{u}^*\right) = \vec{f} - \nabla^* P + \mu\nabla^{*2}\vec{u}^* \ , \tag{9}$$

where ρ is the fluid density, μ the dynamic viscosity, $\vec{u}^*$ the velocity vector, $\vec{f}$ the body force, and $P = p - \rho|\vec{\Omega}\times\vec{r}|^2/2$ the modified pressure by centrifugal force. In present analysis, we assume that the velocity has two components $\vec{u}^* = (u^*, v^*, 0)$. The body force for EOF is electrical field force along x^*-axis and can be expressed as

$$\vec{f} = (-\rho_e E, 0, 0) \ \text{ with } \ \rho_e = -\varepsilon\frac{d^2\psi^*}{dz^{*2}} \ , \tag{10}$$

where ρ_e is the charge density of the electrolyte and E is the constant electric field applied in the x^*-axis direction. Similar to the assumption in Ref. [28], considering the unsteady effects, the transient velocity fields depend only on z^* and t^*. Ignoring the influence of pressure gradient, the unsteady Navier-Stokes Eq. (9) can be simplified as

$$\frac{\partial u^*}{\partial t^*} - 2\Omega v^* = -\frac{1}{\rho}\rho_e E + \nu\frac{\partial^2 u^*}{\partial z^{*2}} \ , \tag{11}$$

https://doi.org/10.1017/jmech.2016.9 Published online by Cambridge University Press

$$\frac{\partial v^*}{\partial t^*} + 2u^* = \nu \frac{\partial^2 v^*}{\partial z^{*2}} . \tag{12}$$

Furthermore, introducing the following dimensionless parameters

$$u = \frac{u^*}{U_{eo}} , \ t = \frac{t^*}{1/\Omega} , \ U_{eo} = \varepsilon E \zeta / \mu , \tag{13}$$

where U_{eo} is classical EOF velocity through microchannel without rotating effect. The dimensionless Eqs. (11) and (12) yield

$$\frac{\partial^2 u}{\partial z^2} + 2\omega v - \omega \frac{\partial u}{\partial t} = -K^2 \psi , \tag{14}$$

$$\frac{\partial^2 v}{\partial z^2} - 2\omega u - \omega \frac{\partial v}{\partial t} = 0 , \tag{15}$$

where $\nu = \mu / \rho$ and $\omega = \Omega H^2 / \nu$ is a nondimensional measure of frequency in the rotating frame. The rotation and the electric field are suddenly applied, thus the initial conditions of Eqs. (14) and (15)

$$u = v = 0 , \ t = 0 , \tag{16}$$

and the no-slip boundary conditions

$$u = v = 0 , \ z = \pm 1 . \tag{17}$$

For the two-dimensional velocity fields, a complex value function $\chi(z, t) = u + iv$ (i is imaginary unit) is introduced. The real part of χ is the velocity in x direction and its imaginary part is the velocity in y direction. Equations (14) and (15) can be combined into a single equation

$$\omega \frac{\partial \chi}{\partial t} + 2i\omega \chi - \frac{\partial^2 \chi}{\partial z^2} = K^2 \psi , \tag{18}$$

and the initial boundary value conditions become

$$\chi = 0 , \ t = 0 , \tag{19}$$

$$\chi = 0 , \ z = \pm 1 . \tag{20}$$

Equation (18) for rotating EOF system represents the balance among the viscous, the Coriolis, the inertia and the electrostatic force.

In order to obtain the solution of the unsteady problem (18), the method of Laplace transform can be employed by the definition

$$\tilde{\chi}(z, s) = L\left[\chi(z, t)\right] = \int_0^\infty \chi(z, t)\, e^{-st} dt . \tag{21}$$

Substituting Eq. (8) into Eq. (18), then performing Laplace transforms of Eq. (18) and utilizing initial condition (19) gives

$$\frac{\partial^2 \tilde{\chi}}{\partial z^2} - (2i + s) \operatorname{Re} \tilde{\chi} = -\frac{K^2}{s} \frac{\cosh Kz}{\cosh K} , \tag{22}$$

$$\tilde{\chi} = 0 , \ z = \pm 1 . \tag{23}$$

Equation (22) is a linear inhomogeneous ODE, and its solution can be expressed by the sum of a general solution corresponding to homogeneous equation and a special solution. The final transformed complex velocity can be expressed as

$$\tilde{\chi}(z, s) = \frac{K^2}{s\left[K^2 - (2i + s)\,\omega\right]} \left[\frac{\cosh \sqrt{(2i + s)\,\omega} z}{\cosh \sqrt{(2i + s)\,\omega}} - \frac{\cosh(Kz)}{\cosh K} \right] . \tag{24}$$

Then, the complex velocity is determined by using Laplace inversion theorem

$$\chi(z, t) = L^{-1}\left[\tilde{\chi}(z, s)\right] = \frac{1}{2\pi i} \int_{c-i\infty}^{c+i\infty} \tilde{\chi}(z, s)\, e^{st} ds , \tag{25}$$

where c is a positive real constant. Usually the Cauchy residue theorem is used to evaluate the integral of Eq. (25), whose value can be expressed by the sum of the residues of $\tilde{\chi}(z, s)\, e^{st}$ at the poles inside contour. Clearly, the integrand has simple poles

$$s = 0 , \ s = \frac{K^2}{\omega} - 2i \ \text{ and}$$

$$s_n = -\frac{(n - 1/2)^2 \pi^2}{\omega} - 2i , \ n = 0 , \pm 1 , \pm 2 , \pm 3 , \cdots$$

The residues of the integrand at these poles are respectively

$$\operatorname{Re} s(0) = \lim_{s \to 0} s e^{st} \tilde{\chi}(z, s) = \frac{K^2}{K^2 - 2i\omega} \left(\frac{\cosh \sqrt{2i\omega} z}{\cosh \sqrt{2i\omega}} - \frac{\cosh Kz}{\cosh K} \right) ,$$

$$\operatorname{Re} s\left(\frac{K^2}{\omega} - 2i \right) = \lim_{s \to \frac{K^2}{\omega} - 2i} \left(s - \frac{K^2}{\omega} + 2i \right) e^{st} \tilde{\chi}(z, s) = 0 ,$$

$$\operatorname{Re} s(s_n) = -\lim_{s \to s_n} \frac{K^2}{s\left[K^2 - (2i + s)\,\omega\right]} \times e^{st} \lim_{s \to s_n} \frac{\cosh \sqrt{(2i + s)\,\omega} z}{\cosh \sqrt{(2i + s)\,\omega}} (s - s_n)$$

$$= \frac{(-1)^n (2n - 1)\, \pi K^2 \cosh\left((n - 1/2)\, \pi z\right)}{\left[(n - 1/2)^2 \pi^2 + 2i\omega\right]\left[(n - 1/2)^2 \pi^2 + K^2\right]} e^{-\left[\frac{(n-1/2)^2 \pi^2}{\omega} + 2i\right] t} .$$

Thus, the inverse Laplace transform gives the eventual complex velocity expression

$$\chi(z, t) = \frac{K^2}{K^2 - 2i\omega} \left(\frac{\cosh \sqrt{2i\omega} z}{\cosh \sqrt{2i\omega}} - \frac{\cosh(Kz)}{\cosh K} \right) + \sum_{n=1}^{\infty} \frac{(-1)^n (2n - 1)\, \pi K^2 \cos\left((n - 1/2)\, \pi z\right)}{\left[(n - 1/2)^2 \pi^2 + 2i\omega\right]\left[(n - 1/2)^2 \pi^2 + K^2\right]} e^{-\left[\frac{(n-1/2)^2 \pi^2}{\omega} + 2i\right] t} . \tag{26}$$

https://doi.org/10.1017/jmech.2016.9 Published online by Cambridge University Press

with the evolution of the time, the rotating EOF velocity attains steady status obtained in Ref. [28]. It can be concluded that our present analysis is valid. With the velocity distributions being known, a transient complex volume flow rate Q per unit width normalized by $\varepsilon E\zeta L/\mu$, can be defined as

$$Q = Q_x + iQ_y = \int_{-1}^{1} \chi dz = \frac{K^2}{K^2 - 2i\omega}\left(\frac{\tanh\sqrt{2i\omega}}{\sqrt{2i\omega}} - \frac{\tanh K}{K}\right) - 4\sum_{n=1}^{\infty}\frac{K^2 \exp\left\{-\left[\frac{(n-1/2)^2\pi^2}{\omega} + 2i\right]t\right\}}{\left[(n-1/2)^2\pi^2 + 2i\omega\right]\left[(n-1/2)^2\pi^2 + K^2\right]}, \tag{27}$$

where the real part Q_x is the EOF rate in the x direction, and the imaginary part Q_y is the EOF rate in the y direction.

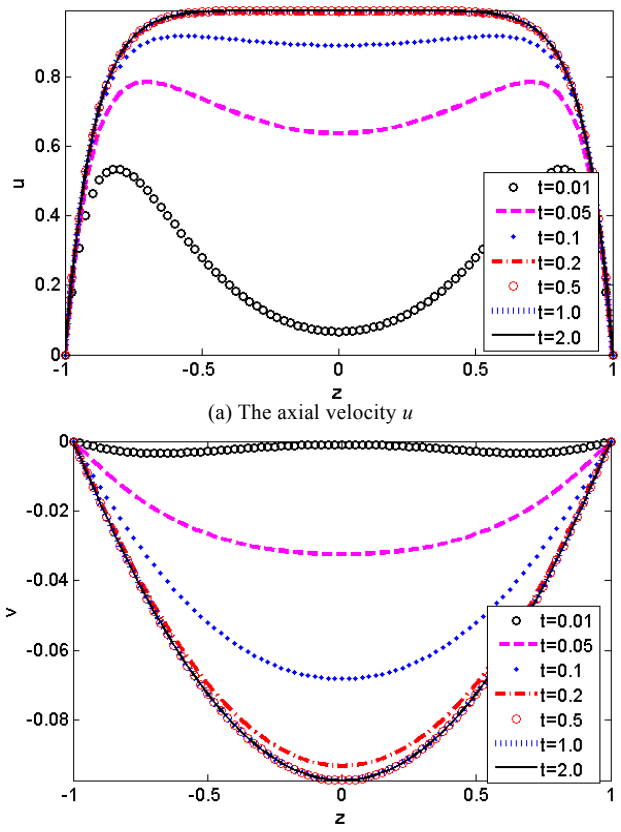
3. RESULTS AND DISCUSSIONS

In the previous sections, analytical solutions were derived for the unsteady rotating EOF velocity, volume flow rate and EO spiral between two microparallel planes. The solution above is for large time t. However, we failed to obtain a solution for small t, which is the inversion of the expansion for large s. They depend greatly on time t, rotating parameter ω and electrokinetic width K. In practical engineering problems of microfluidics, typical parameters are as follows. The half height of microparallel plate is $H = 100\mu m$, and the viscosity of the fluid is $v = 10^{-6}m^2/s$. The speed of rotation is 90 000 rpm in Ref. [28], thus the rotating angle velocity can be up to 9 000 rad/s, and in our paper the rotating angle velocity Ω changes from 0 to 1000 rad/s. Based upon these parametric values, the ω can be evaluated from 0 to 10, and there are no inertial oscillations since we restrict to small ω values. In addition, the typical parametric value of electrokinetic width K changes from 5 to 50.

3.1 Transient Rotating EOF Velocity Profiles

When $K = 20$ and $\omega = 0.1$, 2, 10, Figs. 2 ~ 4 illustrates the transient rotating EOF velocity profiles at different time. It can be seen from Figs. 2 ~ 4 that with the increasing ω, the time of the unsteady rotating flow attaining steady status increases. That is because the stronger rotation applied on the system, the longer time needed to reach a steady state. In addition, the EOF velocity u in axial direction is greatly larger than v in lateral direction when ω is small. However, with ω increasing, the velocities u and v are of the same order of magnitude.

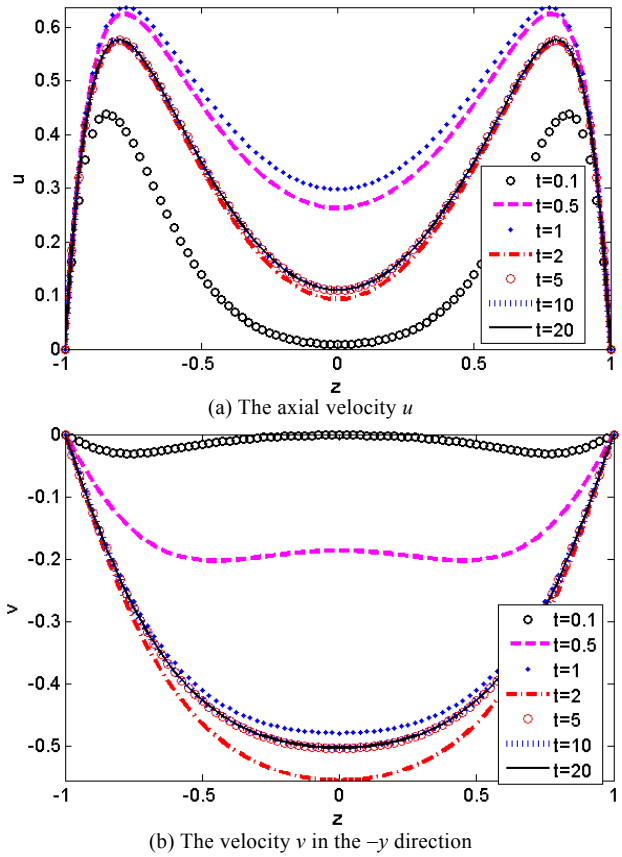
Figures 5 ~ 7 show the variation of unsteady rotating EOF velocity with ω (0.1, 0.3, 1.0, 5.0, 10) for different time $t = 0.01$, $t = 0.1$and $t = 1$. At the center of the channel, the velocities both in x-axis and in y-axis are almost zero when ω is large. When $t = 0.01$ in Fig. 5,



(a) The axial velocity u

(b) The velocity v in the $-y$ direction

Fig. 2 The transient rotating EOF velocity profiles for different t ($K = 20$, $\omega = 0.1$).

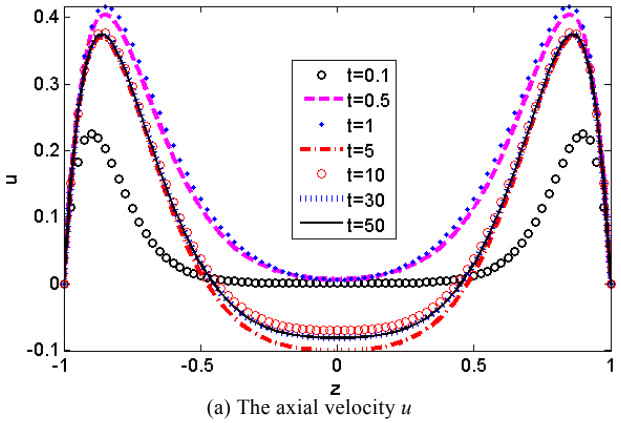


(a) The axial velocity u

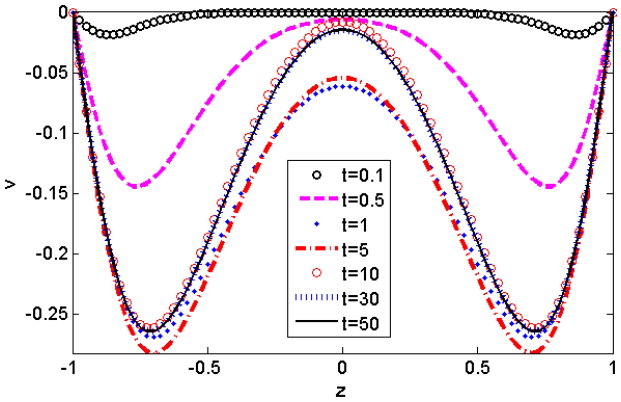
(b) The velocity v in the $-y$ direction

Fig. 3 The transient rotating EOF velocity profiles for different t ($K = 20$, $\omega = 2$).

https://doi.org/10.1017/jmech.2016.9 Published online by Cambridge University Press

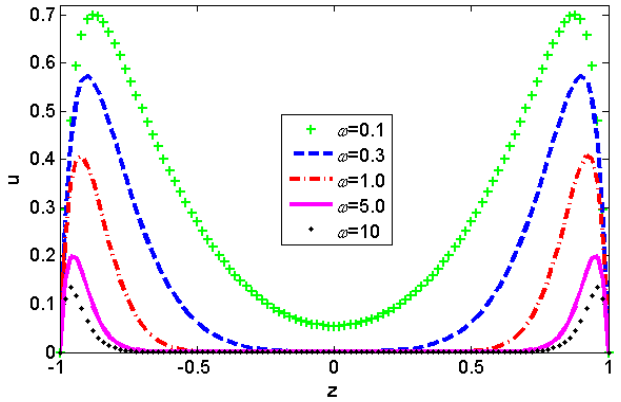


(a) The axial velocity u

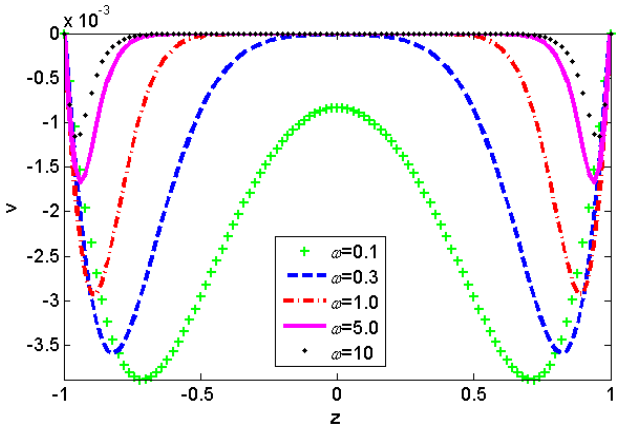


(b) The velocity v in the $-y$ direction

Fig. 4 The transient rotating EOF velocity profiles for different t ($K = 20$, $\omega = 10$).



(a) The axial velocity u



(b) The velocity v in the $-y$ direction

Fig. 5 The transient rotating EOF velocity profiles for different ω ($K = 20$, $t = 0.01$).

with the increase of ω, both the EOF velocities u and v decrease gradually. When $t = 0.1$ in Fig. 6, with the increase of ω, both the EOF velocities u decrease. Near the plates, the velocity v in $-y$-direction increases with ω. However, at the center of the channel, the velocity v reduces with ω. It can be seen from Fig. 7 that the velocity u reduces with ω. Moreover, the velocity v increases with ω near the channel. However, at the center of the channel, the velocity v increases first and then decreases. From Figs. 5 ~ 7, we can find that the velocity u in x-direction is larger than that in y-direction.

Figures 8 ~ 10 depict the variation of rotating EOF velocity with K (5, 10, 20, 50) for different time $t = 0.1$ and $t = 1$ when $\omega = 1$. It can be found both from Figs. 8 and 9 that the center velocity of u is reduced, while the velocities of u and v near the plates increase as the increasing K. Additionally, the lateral velocity v in Fig. 10 will no longer enhance with further increase of K.

3.2 Rotating EOF Volume Flow Rate Profiles

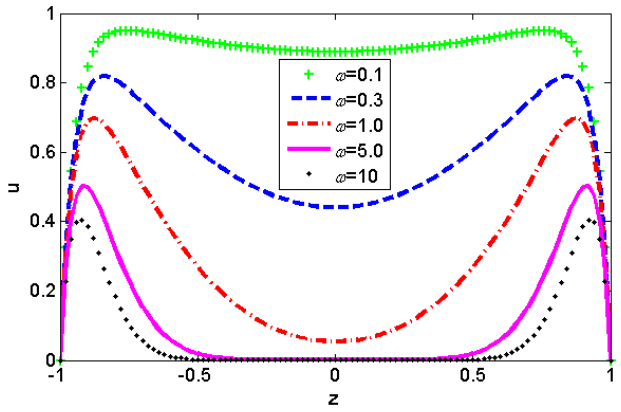
Figure11 illustrates the variation of the volume flow rate in two directions with K when $\omega = 2$ for different times t (0.1, 0.5, 1, 2, 5, 10, 50). With the increasing time (for example, when $t > 10$), the flow rate approximates a steady value both in axial and in lateral directions.

The variation of rotating EOF volume flow rate with ω (0.1, 0.3, 1.0, 5.0, 10) when $t = 0.1$ and $t = 1$ are given in Fig. 12. The volume flow rates in axial direction Q_x and in lateral direction Q_y are reduced with the increasing ω when $t = 0.1$. When $t = 1$, the flow rate in x direction decreases with ω, but the flow rate in $-y$ direction does not change monotonously. For a certain ω, the flow rate enhances with K. However, its change rate becomes small for both two directions at any time.

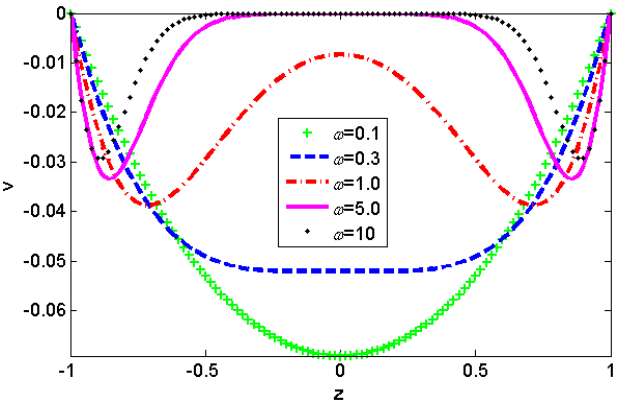
3.3 EO Spiral Orbit

In Fig. 13, we plot the EO Ekman spirals on the u-υ plane for different ω (0.1, 1, 10) at different times t (0.01, 0.1, 3, 30). The Ekman spiral is a structure of currents or winds near a horizontal boundary in which the flow direction rotates as one moves away from the boundary. We can see that if rotating parameter ω is large and the time is small, the spiral is a closed orbit, such as $\omega = 1$, 10 in Fig. 13(a) and $\omega = 10$ in Fig. 13(b). Otherwise, the curves are not closed. For large ω (for example $\omega = 10$), the time needed to reach the steady state is long, thus at the beginning of rotation (time is small), the fluid in the center of the micochannel dose not start to flow, and the velocities at the center are zero in both x and $-y$ direction, at the same time those at the boundary of the channel are also zero, which is the reason why spiral orbit is closed in this case. With the development of time, all the fluid in the channel starts to flow and velocities in the center of the channel cannot be zero, thus the spiral orbit cannot be closed.

https://doi.org/10.1017/jmech.2016.9 Published online by Cambridge University Press

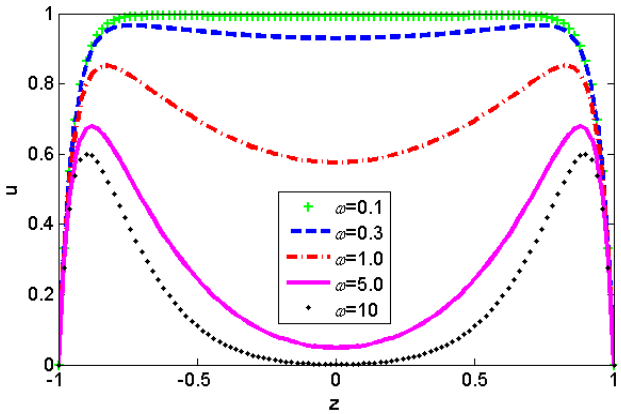


(a) The axial velocity u

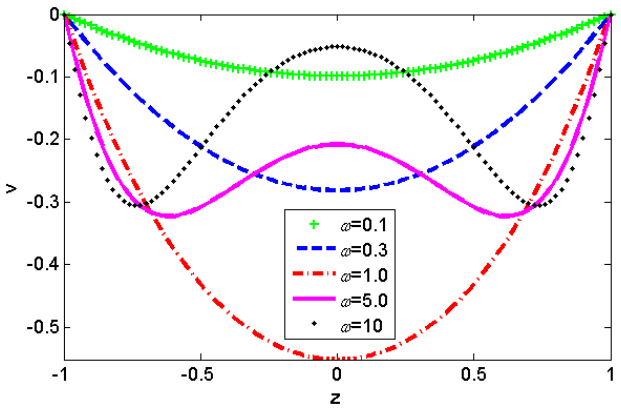


(b) The velocity v in the $-y$ direction

Fig. 6 The transient rotating EOF velocity profiles for different ω ($K = 20$, $t = 0.1$).

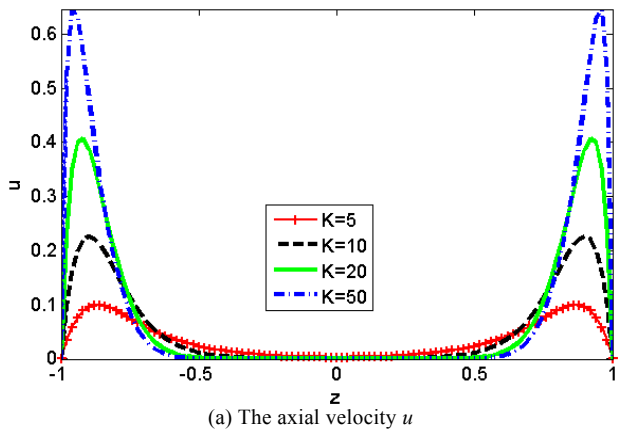


(a) The axial velocity u

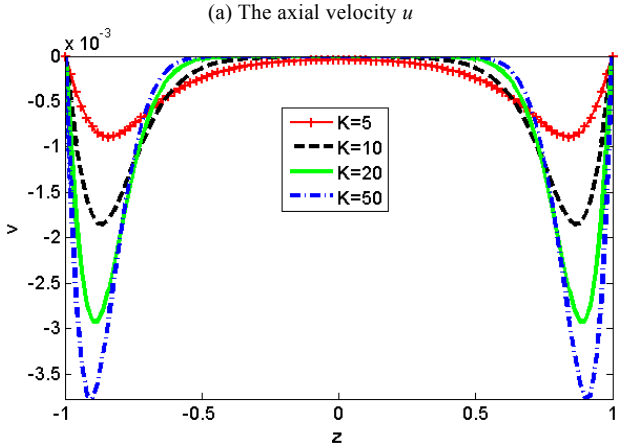


(b) The velocity v in the $-y$ direction

Fig. 7 The transient rotating EOF velocity profiles for different ω ($K = 20$, $t = 1$).

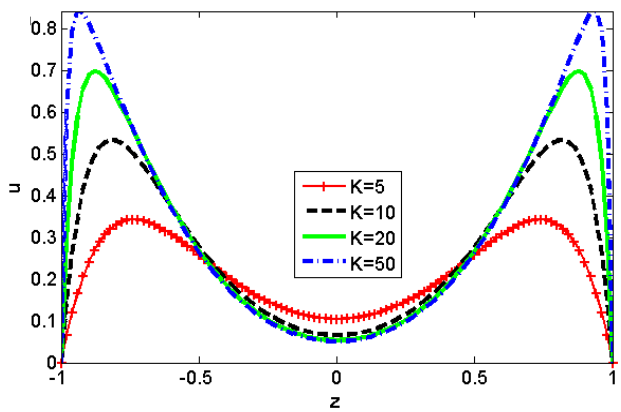


(a) The axial velocity u

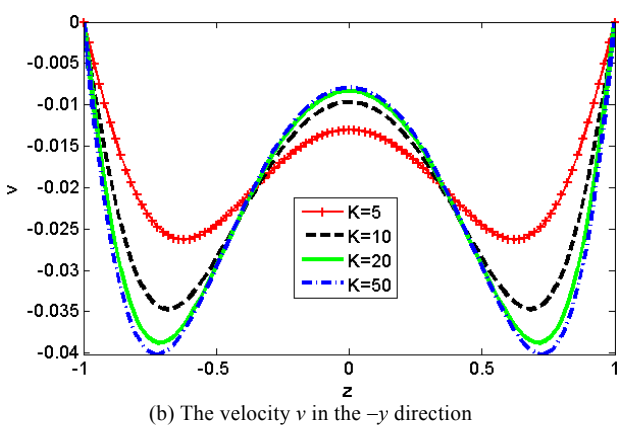


(b) The velocity v in the $-y$ direction

Fig. 8 The transient rotating EOF velocity profiles for different K ($\omega = 1$, $t = 0.01$).



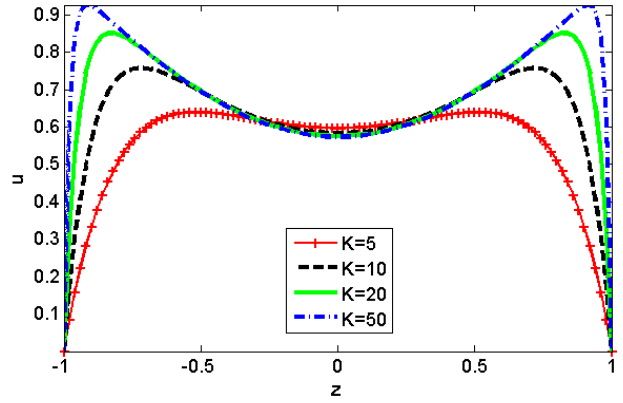
(a) The axial velocity u



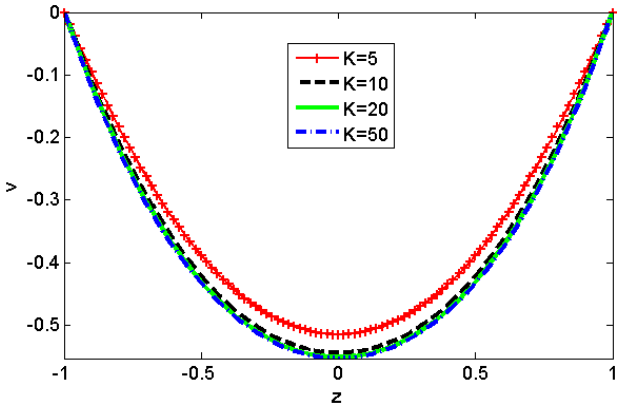
(b) The velocity v in the $-y$ direction

Fig. 9 The transient rotating EOF velocity profiles for different K ($\omega = 1$, $t = 0.1$).

https://doi.org/10.1017/jmech.2016.9 Published online by Cambridge University Press

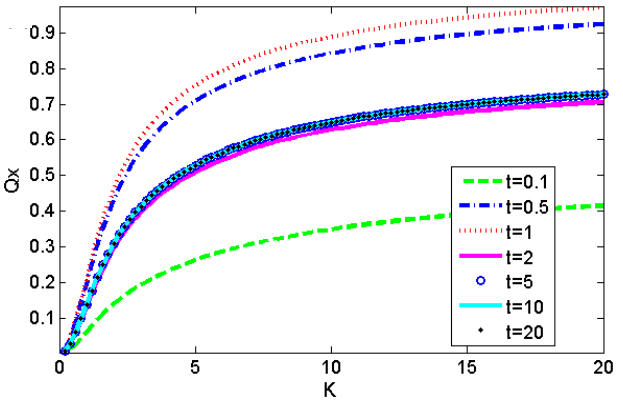


(a) The axial velocity u

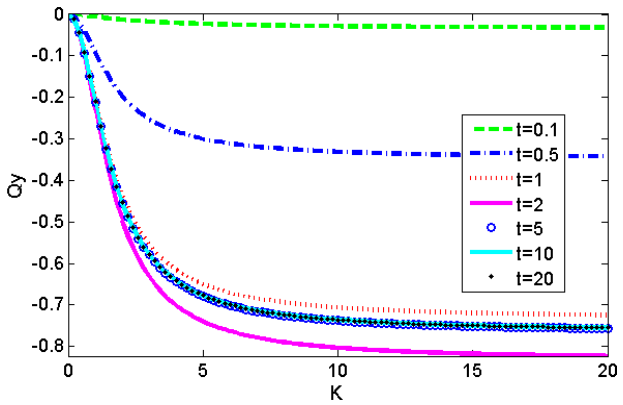


(b) The velocity v in the $-y$ direction

Fig. 10 The transient rotating EOF velocity profiles for different K ($\omega = 1$, $t = 1$).

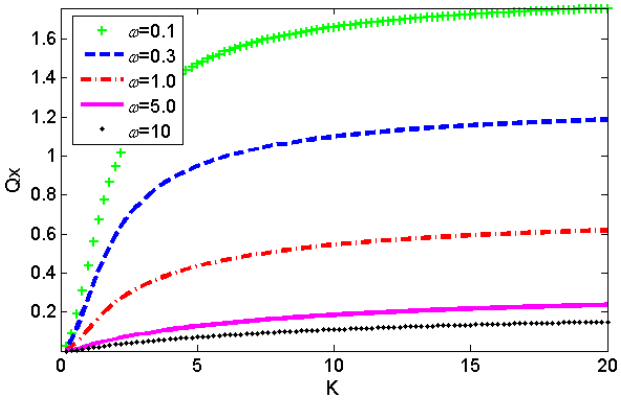


(a) The axial EOF flow rate Q_x

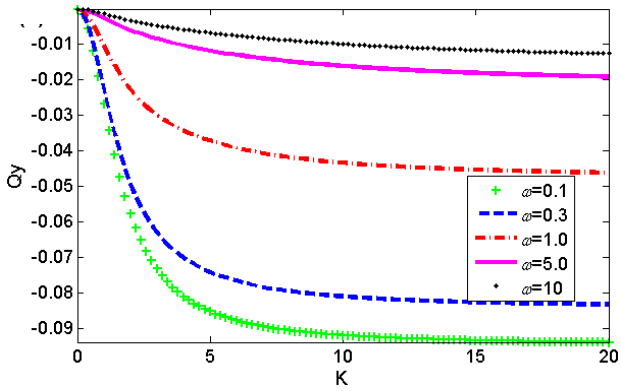


(b) The lateral EOF flow rate Q_y

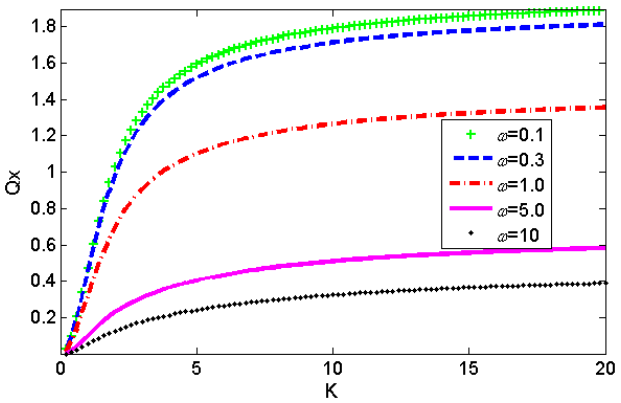
Fig. 11 Transient volume flow rate profiles for different t ($\omega = 2$).



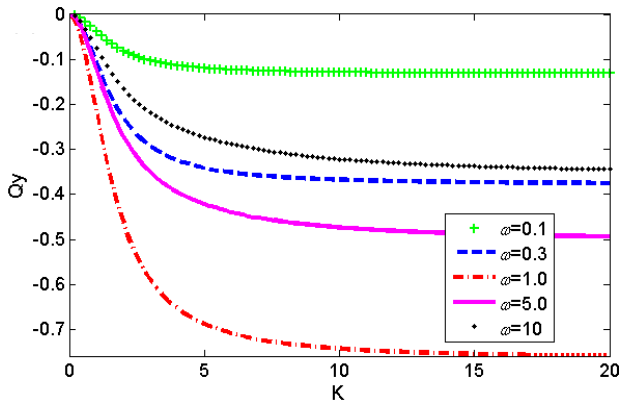
(a) The axial EOF flow rate Q_x when $t = 0.1$



(b) The lateral EOF flow rate Q_y when $t = 0.1$



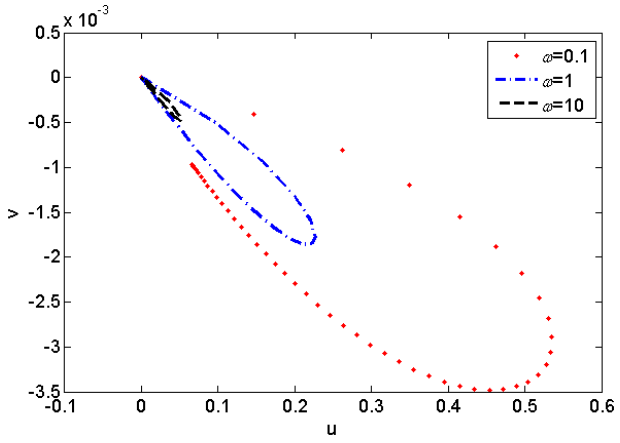
(c) The axial EOF flow rate Q_x when $t = 1$



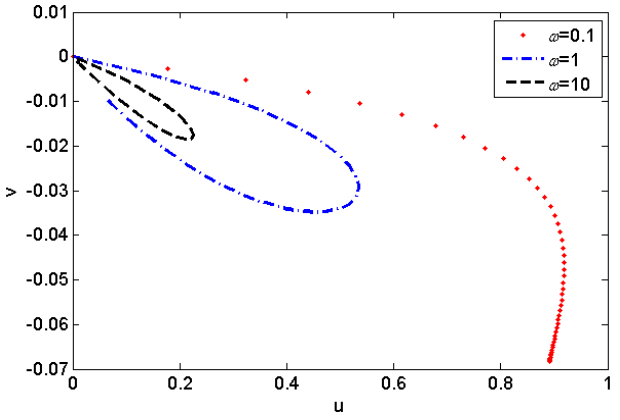
(d) The lateral EOF flow rate Q_y when $t = 1$

Fig. 12 Variation of EOF flow rate with K for different ω.

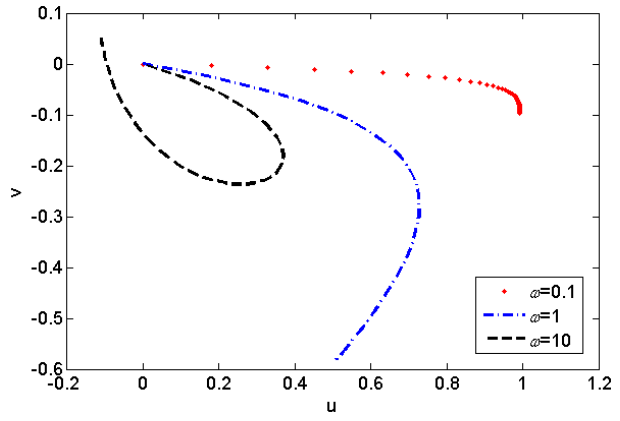
https://doi.org/10.1017/jmech.2016.9 Published online by Cambridge University Press



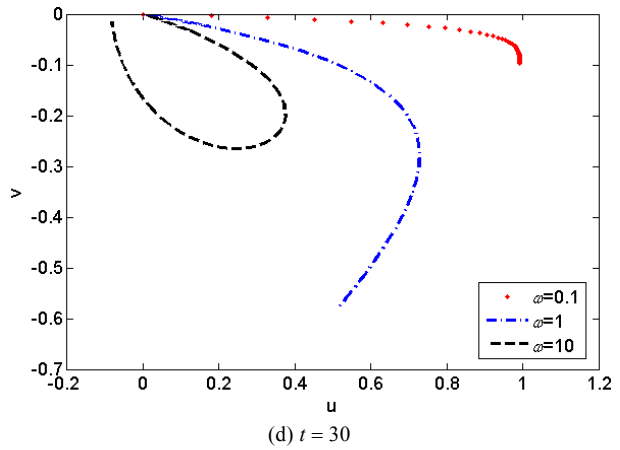
(a) $t = 0.01$



(b) $t = 0.1$



(c) $t = 3$



(d) $t = 30$

Fig. 13 EO Ekman spirals on the u-υ plane for different ω (0.1, 1, 10) at different times t.

4. CONCLUSIONS

The paper presents a study of the unsteady rotating EOF in a channel formed by two charged microparallel plates when the rotation and the axial field are suddenly applied. The effects of electro-kinetic width K and the rotating parameter ω on the unsteady rotating EOF velocity are investigated. The main conclusions are as follows.

From the Figs. 2 ~ 4, we draw a common conclusion that the higher the rotating parameter ω, the longer the time to attain the steady state. At the initial developing step, the velocities both in x direction and in $-y$ direction are reduced with increasing ω. When ω is small, the shape of the lateral velocity profile is parabolic. On the contrary, when ω enlarges, the velocity profiles start to oscillate. The volume flow rates in axial direction Q_x and in lateral direction Q_y are reduced with the increasing ω when t is small. For a larger time, the flow rate in x direction decreases with increasing ω, but the flow rate in $-y$ direction does not change monotonously. Influenced by the two plates in the microchannel, the EO spiral orbit is closed only when rotating parameter is large and the time is small.

ACKNOWLEDGEMENTS

The work was supported by the National Natural Science Foundation of China (Nos. 11472140, 11202092), the Program for Young Talents of Science and Technology in Universities of Inner Mongolia Autonomous Region (No. NJYT-13-A02), and opening fund of State Key Laboratory of Nonlinear Mechanics.

REFERENCES

1. Stone, H. A., Stroock, A. D. and Ajdari, A., "Engineering Flows in Small Devices: Microfluidics Toward a Lab-on-a-Chip," *Annual Review of Fluid Mechanics*, **36**, pp. 381–411 (2004).
2. Erickson, D. and Li, D., "Integrated Microfluidic Devices," *Analytica Chimica Acta*, **505**, pp. 11–26 (2004).
3. Squires, T. M. and Quake, S. R., "Microfluidics: Fluid Physics at the Nanoliter Scale," *Reviews of Modern Physics*, **77**, pp. 977–1026 (2005).
4. Burgreen, D. and Nakache, F. R., "Electrokinetic Flow in Ultrafine Capillary Slits," *Journal of Physical Chemistry*, **68**, pp. 1084–1091 (1964).
5. Rice, C. L. and White, R., "Electrokinetic Flow in a Narrow Cylindrical Capillary," *Journal of Physical Chemistry*, **69**, pp. 4017–4023 (1965).
6. Levine, S., Marriott, J. R., Neale, G. and Epstein, N., "Theory of Electrokinetic Flow in Fine Cylindrical Capillaries at High Zeta Potentials," *Journal of Colloid Interface Science*, **52**, pp. 136–149 (1975).
7. Tsao, H. K., "Electroosmotic Flow Through an Annulus," *Journal of Colloid Interface Science*, **225**, pp. 247–250 (2000).

https://doi.org/10.1017/jmech.2016.9 Published online by Cambridge University Press

8. Kang, Y. J., Yang, C. and Huang, X. Y., "Electroosmotic Flow in a Capillary Annulus with High Zeta Potentials," *Journal of Colloid Interface Science*, **253**, pp. 285–294 (2002).
9. Hsu J. P., Kao C. Y., Tseng, S. J. and Chen, C. J., "Electrokinetic Flow Through an Elliptical Microchannel: Effects of Aspect Ratio and Electrical Boundary Conditions," *Journal of Colloid Interface Science*, **248**, pp. 176–184 (2002).
10. Yang, C. and Li, D., "Analysis of Electrokinetic Effects on the Liquid Flow in Rectangular Microchannel," *Colloids Surface A: Physicochemistry Engineering Aspects*, **143**, pp. 339–353 (1998).
11. Yang, C., Li, D. and Masliyah, J. H., "Modeling Forced Liquid Convection in Rectangular Microchannels with Electrokinetic Effects," *International Journal of Heat and Mass Transfer*, **41**, pp. 4229–4249 (1998).
12. Arulanandam, S. and Li, D., "Liquid Transport in Rectangular Microchannels by Electroosmotic Pumping," *Colloids Surface A: Physicochemistry Engineering Aspects*, **161**, pp. 89–102 (2000).
13. Bhattacharyya, S., Zheng, Z. and Conlish, A. T., "Electro-Osmotic Flow in Two Dimensional Charged Micro- and Nanochannels," *Journal of Fluid Mechamics*, **540**, pp. 247–267 (2005).
14. Bianchi, F., Ferrigno, R. and Girault, H. H., "Finite Element Simulation of an Electroosmotic Driven Flow Division at a T-Junction of Microscale Dimensions," *Analytical Chemistry*, **72**, pp. 1987–1993 (2000).
15. Wang, C. Y., Liu, Y. H. and Chang C. C., "Analytical Solution of Electro-Osmotic Flow in a Semicircular Microchannel," *Physics of Fluids*, **20**, p. 063105 (2008).
16. Chang, C. C. and Wang, C. Y., "Electro-Osmotic Flow in a Sector Microchannel," *Physics of Fluids*, **21**, p. 042002 (2009).
17. Keh, H. J. and Tseng, H. C., "Transient Electrokinetic Flow in Fine Capillaries," *Journal of Colloid Interface Science*, **242**, pp. 450–459 (2001).
18. Kang, Y. J., Yang, C. and Huang, X. Y., "Dynamic Aspects of Electroosmotic Flow in a Cylindrical Microcapillary," *International Journal of Engineering Science*, **40**, pp. 2203–2221 (2002).
19. Sun, Y. J., Jian, Y. J., Chang, L. and Liu, Q. S., "Thermally Fully Developed Electroosmotic Flow of Power-Law Fluids in a Circular Microchannel," *Journal of Mechanics*, **29**, pp. 609–616 (2013).
20. Liu, Q. S., Jian, Y. J. and Yang, L. G., "Alternating Current Electroosmotic Flow of the Jeffreys Fluids Through a Slit Microchannel, " *Physics of Fluids*, **23**, p. 102001 (2011).
21. Liu, Q. S., Jian, Y. J. and Yang, L. G., "Time Periodic Electroosmotic Flow of the Generalized Maxwell Fluids Between Two Microparallel Plates," *Journal of Non-Newtonian Fluid Mechanics*, **166**, pp. 178–186 (2011).
22. Jian, Y. J., Liu, Q. S. and Yang, L. G., "AC Electroosmotic Flow of Generalized Maxwell Fluids in a Rectangular Microchannel," *Journal of Non-Newtonian Fluid Mechanics*, **166**, pp. 1304–1314 (2011).
23. Sun, L. X., Jian, Y. J., Chang, L., Zhang, H. Y. and Liu, Q. S., "Alternating Current Electro-Osmotic Flow of the Maxwell Fluids Through a Circular Micro-Pipe," *Journal of Mechanics*, **29**, pp. 233–240 (2013).
24. Deng, S. Y., Jian, Y. J., Bi, Y. H., Chang, L., Wang, H. J. and Liu, Q. S., "Unsteady Electroosmotic Flow of Power-Law Fluid in a Rectangular Microchannel," *Mechanics Research Communications*, **39**, pp. 9–14 (2012).
25. Li, S. X., Jian, Y. J. and Xie, Z. Y., "Rotating Electro-Osmotic Flow of Third Grade Fluids Between Two Microparallel Plates," *Colloids Surface A: Physicochemistry Engineering Aspects*, **470**, pp. 240–247 (2015).
26. Xie, Z. Y. and Jian, Y. J., "Rotating Electroosmotic Flow of Power-Law Fluids at High Zeta Potential," *Colloids Surface A: Physicochemistry Engineering Aspects*, **461**, pp. 231–239 (2014).
27. Jian, Y. J., Si, D. Q., Chang, L. and Liu, Q. S., "Transient Rotating Electromagnetohydrodynamic Micropumps Between Two Infinite Microparallel Plates," *Chemistry Engineering Science*, **134**, pp. 12–22 (2015).
28. Chang, C. C. and Wang, C. Y., "Rotating Electro-Osmotic Flow over a Plate or Between Two Plates," *Physical Review E*, **84**, p. 056320(2011).

(Manuscript received July 10, 2015,
accepted for publication September 20, 2015.)

https://doi.org/10.1017/jmech.2016.9 Published online by Cambridge University Press